Textures and Microstructures, 1993, Vol. 21, pp. 3–16
Reprints available directly from the publisher.
Photocopying permitted by license only

DETERMINATION OF THE ELASTIC TENSOR OF A TEXTURED LOW-CARBON STEEL

P. SPALTHOFF,* W. WUNNIKE,* C. NAUER-GERHARD* and H. J. BUNGE*

** Department of Physical Metallurgy, Technical University of Clausthal, Germany*

E. SCHNEIDER**

*** Fraunhofer Institute of Nondestructive Testing, Saarbrücken, Germany*

(Received 25 May 1992)

The components of the elastic stiffness tensor of hot rolled low-carbon steel were determined using an ultrasonic pulse-echo-method. They were also calculated on the basis of X-ray texture measurements using the Hill approximation. The maximum deviation between experimental and calculated values is 3.5%. An influence of the slightly anisotropic grain structure on the elastic anisotropy could not be seen.

KEY WORDS Sound velocity, pulse-echo-overlap technique, elastic stiffness tensor, Hill average, low-carbon steel.

INTRODUCTION

The elastic properties of polycrystalline materials depend on the properties of the constitutive crystallites as well as on their arrangement in the polycrystalline structure. Stress equilibrium and strain continuity across the grain boundaries lead to complicated stress and strain distributions, the macroscopic averages of which define the polycrystal elastic constants. If the actual shape, size, orientation and position of each crystallite is known, then the boundary conditions in the grain boundaries can be strictly taken into account and the polycrystal properties can be calculated straight foreward. However, this is usually not the case. Certain statistical assumptions must then be made which lead to various approximative models for the polycrystal constants. In the Reuss model (Reuss, 1929), constant stress is assumed whereas the Voigt model (Voigt, 1928) assumes constant strain throughout the polycrystal. The polycrystal constants are then the simple volume averages of the components of the stiffness and compliance tensor of the individual crystallites, respectively. These assumptions are limiting cases, the actual values must lie between them. In a first approximation, knowing nothing about the microstructure, the average of both these assumptions can be taken, corresponding to the Hill approximation (Hill, 1952). It has been found that this approximation, although theoretically unsatisfactory, agrees with the experimental results within a few percent, which is sufficient for most practical purposes. A theoretically much more satisfactory model was developed by Kröner (Kröner, 1958). In this model a spherical grain is embedded in a polycrystalline matrix

which is considered as a continuum having the average properties of all crystallites. The Voigt–Reuss–Hill approximation as well as the Kröner model were developed for materials with random orientation distribution as well as for textured materials (Bunge, 1968; Kneer, 1965). In the latter case, comparison between experiment and model calculation was mainly done in the rolling plane of rolled metal sheet. However, in a few cases measurements in sample directions covering the whole orientation sphere were also made (see e.g. Durand, 1977; Kern and Wenk, 1985). Youngs modulus measurements in various sample directions may also be expressed in form of the components of the polycrystal elastic tensor. It is the objective of the present paper to compare the macroscopic elastic tensor calculated from texture data with the one obtained from measurements in several sample directions of a polycrystalline textured material.

TEXTURE AVERAGES OF ELASTIC PROPERTIES

The elastic properties of a single crystal can be expressed by Hook's law in two forms (see e.g. Nye, 1975)

$$\sigma_{ij} = C_{ijkl} \cdot \varepsilon_{kl}, \qquad \varepsilon_{ij} = S_{ijkl} \cdot \sigma_{kl} \tag{1}$$

where σ_{ij} and ε_{ij} are the components of the stress and strain tensor respectively, C_{ijkl} and S_{ijkl} are those of the elastic stiffness and compliance tensor. These tensors are inversely related to each other

$$[S_{ijkl}] = [C_{ijkl}]^{-1}. \tag{2}$$

If we consider single crystals then the tensor components are usually referred to the crystal coordinate system. In a polycrystal each crystal has its own crystal coordinate system related to the macroscopic sample coordinate system by the orientation g which may be represented by the transformation matrix $[g_{ij}]$. The tensor components referred to the sample coordinate system can then be expressed by those referred to the crystal axes and the transformation matrix

$$\begin{aligned} C_{ijkl}(g) &= C^0{}_{mnop} \cdot g_{im} \cdot g_{jn} \cdot g_{ko} \cdot g_{lp} \\ S_{ijkl}(g) &= S^0_{mnop} \cdot g_{im} \cdot g_{jn} \cdot g_{ko} \cdot g_{lp} \end{aligned} \tag{3}$$

The Voigt and Reuss averages are defined by

$$\begin{aligned} \bar{C}^V_{ijkl} &= \oint C_{ijkl}(g) \cdot f(g)\, dg \\ \bar{S}^R_{ijkl} &= \oint S_{ijkl}(g) \cdot f(g)\, dg \end{aligned} \tag{4}$$

Where the integral is taken over the whole orientation space. Finally, the Hill average can be written

$$\begin{aligned} \bar{C}^H_{ijkl} &= \tfrac{1}{2}[\bar{C}^V_{ijkl} + \bar{C}^R_{ijkl}] \\ \bar{S}^H_{ijkl} &= \tfrac{1}{2}[\bar{S}^V_{ijkl} + \bar{S}^R_{ijkl}] \end{aligned} \tag{5}$$

Strictly speaking, the two approximations in Eq. (5) are not identical. They are not exactly related to each other by Eq. (2). Nevertheless, the difference between them may be neglected compared with the experimental errors.

The single crystal tensors $C^0_{mnop}S^0_{mnop}$ must reflect crystal symmetry whereas the polycrystal values $\bar{C}^H_{ijkl}$ and $\bar{S}^H_{ijkl}$ correspond to sample symmetry. Usually, the symmetries are expressed in the matrix representation of the elastic constants rather than in the tensor representation. Hence, C^0_{mnop} and S^0_{mnop} are replaced by C^0_{ij} and S^0_{ij} and $\bar{C}^H_{ijkl}$ and $\bar{S}^H_{ijkl}$ by $\bar{C}^H_{ij}$ and $\bar{S}^H_{ij}$ respectively (see e.g. Nye, 1975). In the present case, crystal symmetry was cubic and the sample has the orthorhombic symmetry of rolled sheet. Hence, only three respectively nine matrix components are symmetrically independent. These are C^0_{11}, C^0_{12}, C^0_{44} for the single crystal and $\bar{C}^H_{11}$, $\bar{C}^H_{22}$, $\bar{C}^H_{33}$, $\bar{C}^H_{12}$, $\bar{C}^H_{13}$, $\bar{C}^H_{23}$, $\bar{C}^H_{44}$, $\bar{C}^H_{55}$, $\bar{C}^H_{66}$ for the polycrystal.

The texture $f(g)$ can be represented in the form of a series expansion

$$f(g) = \sum_{l=0}^{L} \sum_{\mu=1}^{M(l)} \sum_{\nu=1}^{N(l)} C_l^{\mu\nu} \cdot \dot{T}_l^{\mu\nu}(g) \tag{6}$$

which also must reflect crystal and sample symmetry (see e.g. Bunge, 1982). The first one determines the number $M(l)$ of possible values of the index μ, while the latter determines the number $N(l)$ of values of the index ν. Furthermore, the integrals in Eq. (4) are integrals over fourth-order functions. Hence, they can be completely expressed in terms of texture coefficients $C_l^{\mu\nu}$ with l-values up to four. In the case of cubic crystal symmetry and orthorhombic sample symmetry, these are only three coefficients, namely C_4^{11}, C_4^{12}, C_4^{13} (see e.g. Bunge, 1968). The nine polycrystal constants specified above are thus expressed in terms of three single crystal constants and three texture coefficients which amounts to six independent quantities. It is thus seen, that in the case of an orthorhombic *poly*crystal only six of the nine components can really be independent (in contrast to orthohombic single crystals which may really have nine independent components).

ELASTIC WAVES IN ANISOTROPIC MEDIA

The most precise evaluation of elastic constants is based on the velocities of ultrasonic waves propagating the material of interest along different sample directions. In each sample direction three different sound velocities must be distinguished depending on the polarization of the sound wave. Waves travelling along symmetry axes may either be longitudinally polarized or they may have one of two different transversal polarizations. In other directions polarization is neither exactly longitudinal nor exactly transversal. Nevertheless, quasi-longitudinal and quasi-transversal waves can be distinguished.

In the case of orthohombic symmetry we consider two types of sample directions i.e. directions parallel to one of the orthohombic axes, which may then be chosen to be the X_1-axis, and directions perpendicular to one of these axes, e.g. directions in the X_2-X_3 plane. In the latter case, the direction is further specified by its angle θ towards X_2. For these cases, the following expressions are obtained for the various wave velocities (see e.g. Green, 1973)

$$\rho^2 \cdot v^2 \begin{cases} = C_{11} & \text{longitudinal} \\ = C_{66} & \text{transversal pol.} \parallel X_2 \\ = C_{55} & \text{pol.} \parallel X_3 \end{cases} \tag{7}$$

$$\rho^2 \cdot v^2 \begin{cases} = \tfrac{1}{2}(B + \phi) & \text{quasilongitudinal} \\ = a^2(C_{66} - C_{55}) + C_{55} & \text{quasitransversal pol.} \parallel X_1 \\ = \tfrac{1}{2}(B - \phi) & \text{pol.} \perp X_1 \end{cases} \tag{8}$$

where

$$a = \sin\theta \tag{9}$$

$$\begin{aligned}\phi = [&a^4 \cdot C_{22}^2 + (1-a^2)^2 \cdot C_{33}^2 + (1-2a^2)^2 \cdot C_{44}^2 \\ &- 2a^2 \cdot (1-a^2) \cdot C_{22} \cdot C_{33} + 2a^2 \cdot (1-2a^2) \cdot C_{22} \cdot C_{44} \\ &- 2 \cdot (1-a^2) \cdot (1-2a^2) \cdot C_{33} \cdot C_{44} + 4a^2 \cdot (1-a^2) \cdot (C_{23} - C_{44})^2]^{1/2}\end{aligned} \tag{10}$$

$$B = a^2 \cdot (C_{22} - C_{33}) + C_{33} + C_{44}. \tag{11}$$

Expressions for waves travelling in X_2 and X_3 or in the X_3–X_1 or X_1–X_2 plane are similarly obtained by cyclic exchange of the indices 1 2 3 and 4 5 6, respectively.

In the case of orthorhombic symmetry, all nine elastic constants can thus be obtained from time of flight measurements in directions of these two types. The constants C_{ii} can be obtained directly from the very simple expressions Eq. (7), whereas those of the type C_{ij} are obtained by solving the system of equations Eq. (8). It will be seen later on that this leads to a somewhat higher uncertainty of these latter constants.

MATERIAL AND EXPERIMENTAL PROCEDURE

The material used was a low-carbon steel with a composition given in Table 1. After continuous casting the material was hot rolled at 820°C (coiling temperature 550°C) to a final thickness of 18.3 mm. The material had a fine-grained microstructure shown in Figure 1a–c. The average grain size in the three main directions was determined by the linear intercept method. The results are given in Table 2.

Samples for the ultrasonic investigations were prepared as shown in Fig. 2. They were bars of 35 mm lengths with square cross-section and the longitudinal axis at different angles towards the rolling direction. In one set the side faces were parallel and perpendicular to the rolling plane. In the other set they were under 30 degrees. In the first set, the short axes were 16.5 mm, in the second one 12 mm. Hence, in both sets the near-surface region of the hot rolled material was not included in the samples.

The ultrasonic velocities have been evaluated from the results of ultrasonic times-of-flight measurements and of measurements of the samples dimensions. The times-of-flight have been measured using the pulse-echo-overlap technique. The measuring system consists of an ultrasonic transmitter-receiver and a time-of-flight measuring unit with a 500 MHz temperature stabilized time reference (Herzer, Schneider, 1989).

Piecoelectric ultrasonic transducers for longitudinal and linearely polarized shear waves with 10 MHz and 5 MHz center frequencies, respectively have been

Table 1 Chemical composition (weight-%)

C	*Si*	*Mn*	*P*	*S*	*N*	*Al*	*Nb*	*Cu*	*Mo*	*As*	*Zr*
0.04	0.19	1.50	0.014	0.007	0.0068	0.051	00.07	0.03	0.35	0.02	0.08

(a)

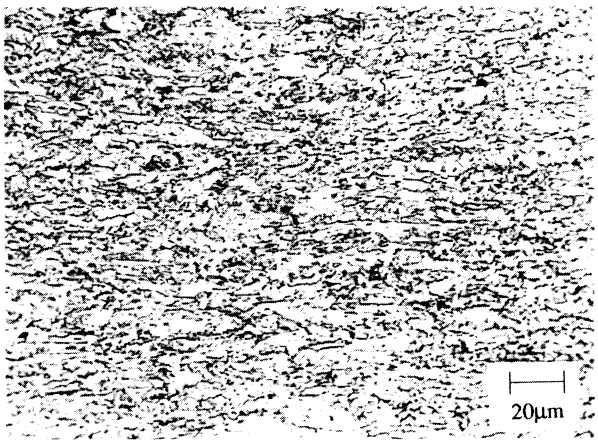

(b)

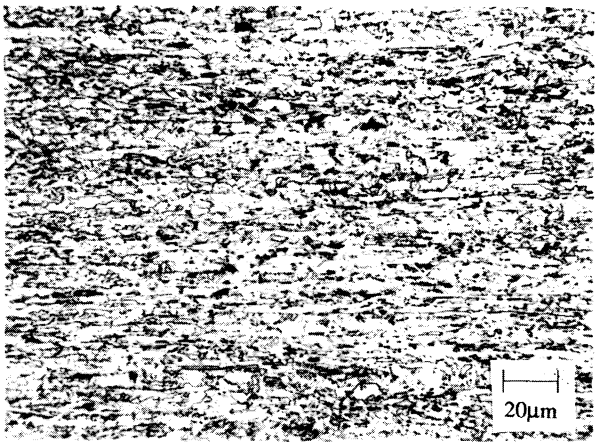

(c)

Figure 1 Metallographic sections of the used steel. The section plane is perpendicular to: (a) Rolling direction RD, (b) Transverse direction TD, (c) Normal direction ND.

Table 2 Average grain size [μm]

RD	*TD*	*ND*
14	11	7

used. The different center frequencies have been chosen to get the same wavelengthes of about 0.6 mm for both, the longitudinal and the transversal waves. The lengthes of the ultrasonic pulses were four wavelengthes in both cases.

The accuracy of the time-of-flight measurements was better than $\pm 1\,ns$, corresponding to a relative accuracy of better than $\pm 0.01\%$. The measurements have been repeated several times in order to minimize inaccuracies caused by the coupling conditions of the ultrasonic probes to the samples. The reproducebility was found to be within $\pm 0.03\%$.

The linear dimensions of the samples have been measured using a micrometer; the inaccuracy of the readings was less than ± 0.003 mm or $\pm 0.03\%$. Thus, the relative accuracy of the velocities is within $\pm 0.06\%$.

With the samples shown in Figure 2 a total of $8 \times 3 \times 3 = 72$ velocities were measured of which 60 belong to the two categories given in Eqs. (7) and (8). The elastic constants were then evaluated using a specially written computer programm (Wunnicke 1986). Since the number of measured velocity values was higher than the number of unknown elastic constants, the relative errors of the latter ones could be estimated.

Texture measurements were carried out using the oblique-section technique (see e.g. Welch, 1980). Hence, the obtained texture corresponds to the volume average. This corresponds to the ultrasonic measurements which are also volume averages. The measurements were done with an automatic texture diffractometer ATEMA-C using Co–Kα radiation. Scanning was done in steps of $\Delta\alpha = 5°$, $\Delta\beta = 3.6°$ up to $\alpha_{max} = 70°$. The original measurements were taken on an oblique-section, the normal direction of which forms equal angles with respect to RD, TD, ND. The obtained pole figures (200), (220) and (211) were then transformed into the coordinate system of the three main sample directions. From these pole figures, the orientation distribution function, ODF, was calculated using the series expansion method based upon complete pole figures, including the zero-range method for the coefficients of odd order.

RESULTS

The pole figures are given in Figure 3a–c. The ODF is shown in Figure 4. Its maximum densities of 8.95 and 8.4, respectively, are reached in the orientations $\sim\{212\}\langle 221\rangle$ and $\sim\{332\}\langle 113\rangle$, respectively. For comparison with physical properties in the three main directions RD, TD and ND, the three inverse pole figures are useful. They are given in Figure 5. The calculation of the texture averages is based on the series expansion coefficients $C_l^{\mu\nu}$ of fourth order. These are given in Table 3. The measured ultrasonic velocities are given in Table 4. The

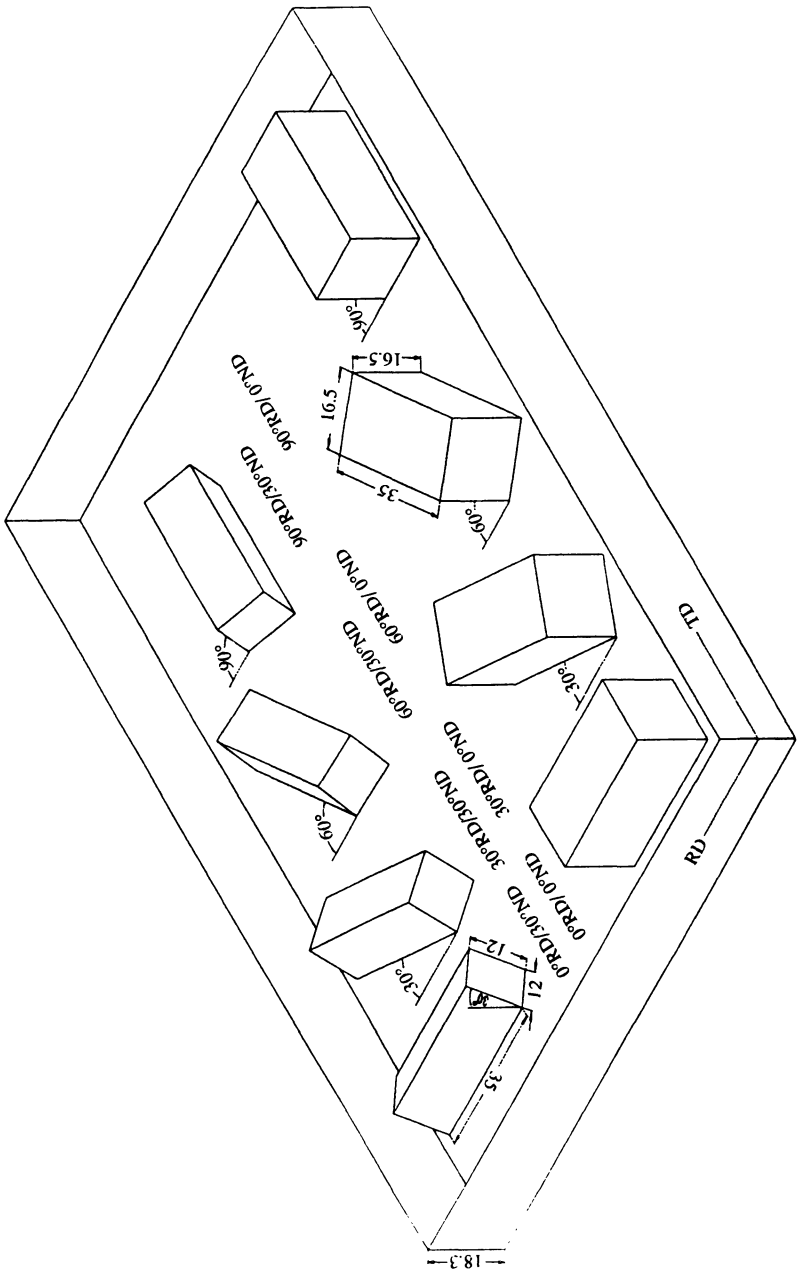

Figure 2 Schematic drawing of the shape and orientation of samples for ultrasonic measurements.

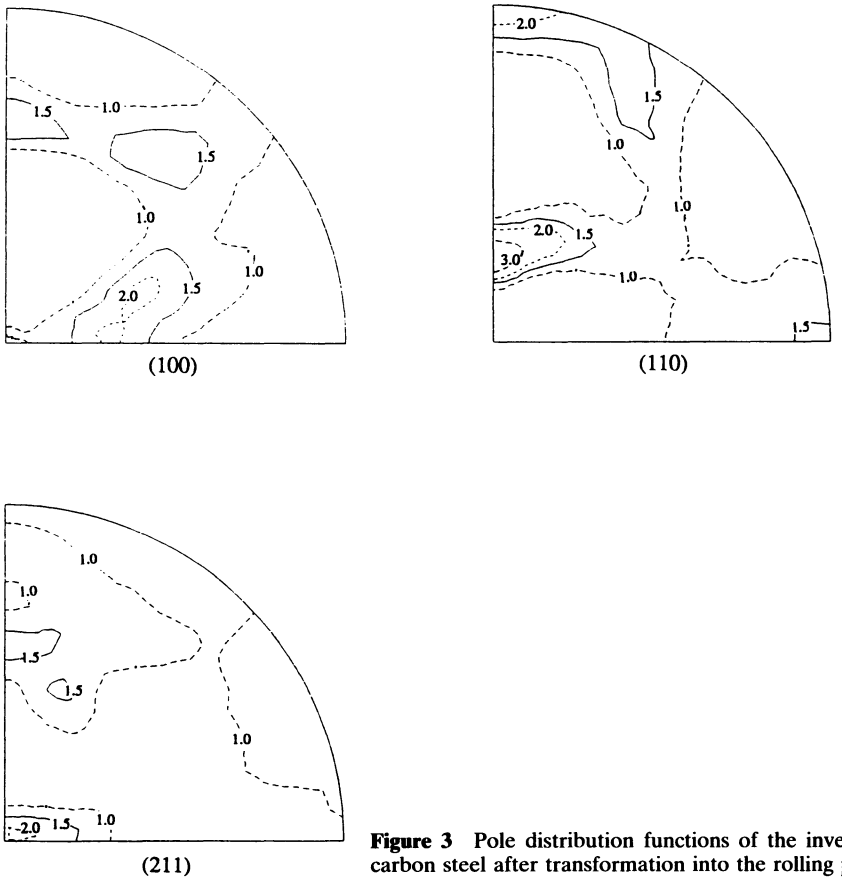

Figure 3 Pole distribution functions of the investigated low-carbon steel after transformation into the rolling plane.

used single crystal elastic constants are $C_{11} = C_{22} = C_{33} = 229000\,\text{N/mm}^2$, $C_{44} = C_{55} = C_{66} = 115000\,\text{N/mm}^2$ and $C_{12} = C_{13} = C_{23} = 134000\,\text{N/mm}^2$. The polycrystal elastic constants are given in Table 5. The ones obtained from ultrasonic measurements are least squares approximations to the sound velocities of different sample directions. This allows the estimation of the standard deviation. It is seen that the uncertainty in the values C_{ij} is much higher than that of the C_{ii}. For the values obtained from texture measurements, the error estimation is much more difficult. Hence, error values are not given in this case. The differences between ultrasonic and texture values are plotted graphically in Figure 6. In Figure 6a the Voigt, Reuss and Hill values are shown whereas Figure 6b shows the Hill averages in a smaller scale. It is seen that the maximum deviation is below 4%. Comparison can also be made in terms of Young's modulus calculated in the three main sample planes X_1-X_2, X_1-X_3, X_2-X_3 (Figure 7) using the coefficients of Table 5. The results are thus linear sections of the Young's modulus surface.

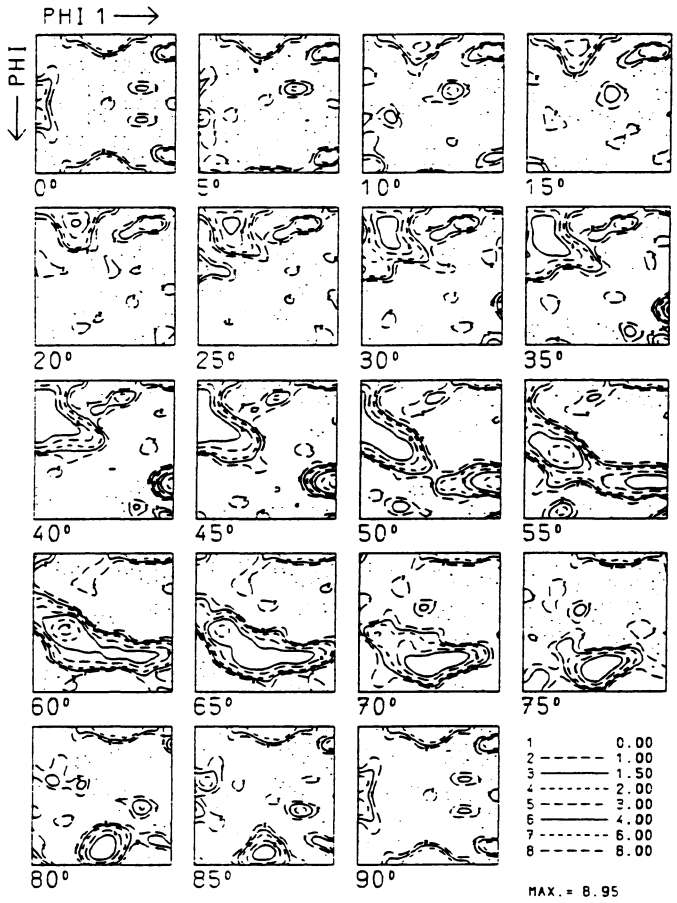

Figure 4 The complete orientation distribution function calculated from the pole figures shown in Figure 3.

DISCUSSION

The elastic properties of textured polycrystals were considered here in the approximation of the Hill average, Eq. (5). This approximation is assumed to be applicable in the case of an equiaxed grain structure. However, non-equiaxed grain shapes may cause deviations from it. For example, in the case of long parallel cylindrical grains, Young's modulus in the axis direction should be near to the Voigt approximation whereas for plate-like grains in the stacking direction the Reuss approximation is to be expected. Hence, an anisotropic grain structure as observed in the present material should influence the actual polycrystal properties. If these are expressed in terms of the polycrystal elastic tensor, then the different tensor components should be modified differently. In the present

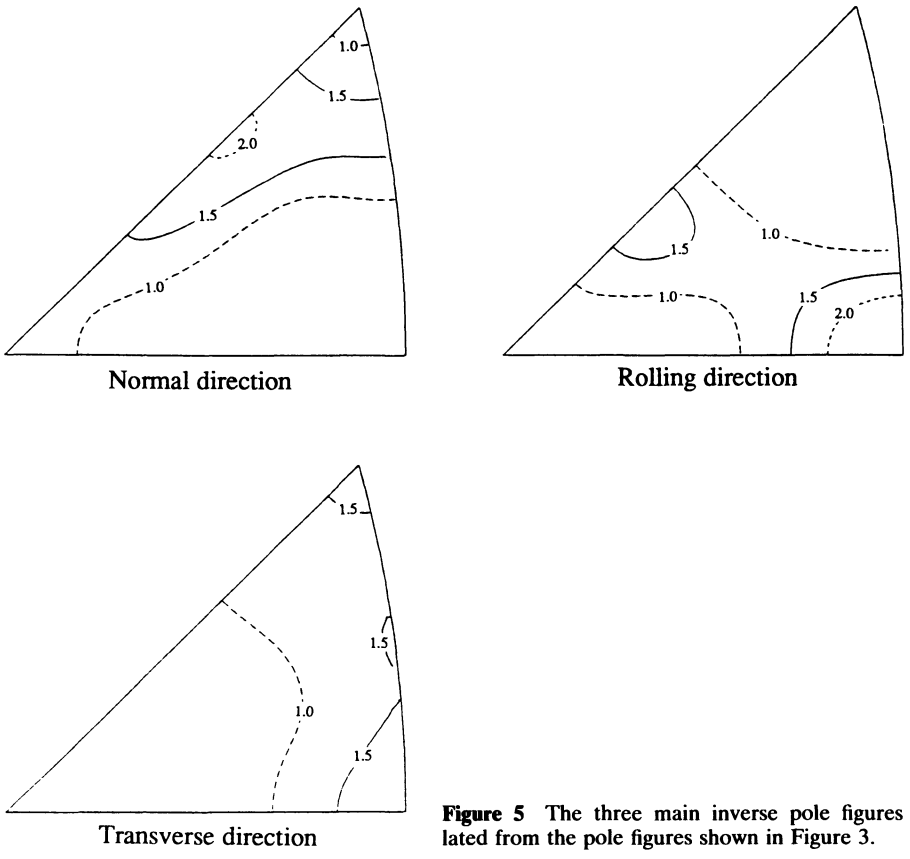

Figure 5 The three main inverse pole figures calculated from the pole figures shown in Figure 3.

case the average grain size was found to be only slightly different in rolling and transverse direction. However, in normal direction it deviated by a factor of two. The influence of grain structure on the elastic anisotropy is thus mainly expected in the normal anisotropy and not in the planar anisotropy. This situation is often observed in grain structures which have been formed by a rolling process (in the present case by hot rolling). It is much easier to measure Young's modulus in the rolling plane than in directions out of this plane. Hence, Young's moduli measured in the rolling plane were often compared with those calculated according to the Hill approximation. With the particular type of microstructure mentioned above the strongest deviations are to be expected in normal direction.

Table 3 Fourth order texture coefficients

C_{11}^4	C_{12}^4	C_{13}^4
−0.3020	−1.1141	−0.2867

Table 4 Ultrasonic velocities [10^3m/s]

Sample	0° *ND*				30° *ND*			
	Wave	*pol* = Y1	Y2	Y3	*Wave*	*pol* = Y1	Y2	Y3
0° RD	Y1 = 100	5·927	3.147	3.265	Y1 = 100	5.933	3.118	3.260
	Y2 = 010	3.157	6.032	3.128	Y2 = 0vu	3.180	5.918	3.289
	Y3 = 001	3.288	3.147	5.922	Y3 = 0ūv	3.260	3.286	5.874
30° RD	Y1 = vu0	5.870	3.236	3.228	Y1 = vu0	5.870	3.230	3.218
	Y2 = ūv0	3.166	5.901	3.187	*Y2 = x̄yu	3.354	5.894	3.172
	Y3 = 001	3.289	3.148	5.929	*Y3 = zx̄v	3.268	3.233	5.909
60° RD	Y1 = uv0	5.948	3.255	3.161	Y1 = uv0	5.959	3.257	3.159
	Y2 = v̄u0	3.253	5.895	3.275	*Y2 = ȳx0	3.250	5.931	3.176
	Y3 = 001	3.146	3.284	5.928	*Y3 = xz̄v	3.168	3.242	5.958
90° RD	Y1 = 010	5.942	3.151	3.132	Y1 = 010	6.027	3.118	3.131
	Y2 = 1̄00	3.141	5.934	3.271	Y2 = v̄0u	3.148	5.965	3.211
	Y3 = 001	3.147	3.291	5.929	Y3 = u0v	3.136	3.234	5.970

u = cos 60°; v = sin 60°; x = $\sqrt{(3/4)}$; y = 3/4; z = 1/4.
* Value not used.

In the present measurements an effect of this type could not be observed, at least not exceeding the experimental accuracy of a few percent which is mainly determined by the accuracy of the texture measurement.

In an earlier investigation in cold rolled copper (Bunge, Öhme and Günther, 1970) a stronger deviation in the normal anisotropy was found than in the planar anisotropy. This effect did not occur in recrystallized copper. It was assumed that this effect was due to the influence of grain shape. Considering the present results, these conclusions were not confirmed here.

In addition to an anisotropic microstructure, the anisotropy of elastic properties may also be influenced by internal residual stresses. Because of the stress-

Table 5 Elastic constants [N/mm^2]

C_{ij}	Reuss	Voigt	Hill	*ultrasonic*
C_{11}	261270	280660	270070	274400 ± 181
C_{12}	115230	105630	110850	110546 ± 5588
C_{13}	120500	110710	116080	115029 ± 1848
C_{22}	271440	290450	280160	280800 ± 670
C_{23}	110330	100920	105990	105225 ± 2104
C_{33}	266160	285370	274930	273917 ± 175
C_{44}	67790	81920	74190	76817 ± 78
C_{55}	77160	91710	83810	83845 ± 109
C_{66}	72000	86630	78640	77343 ± 109

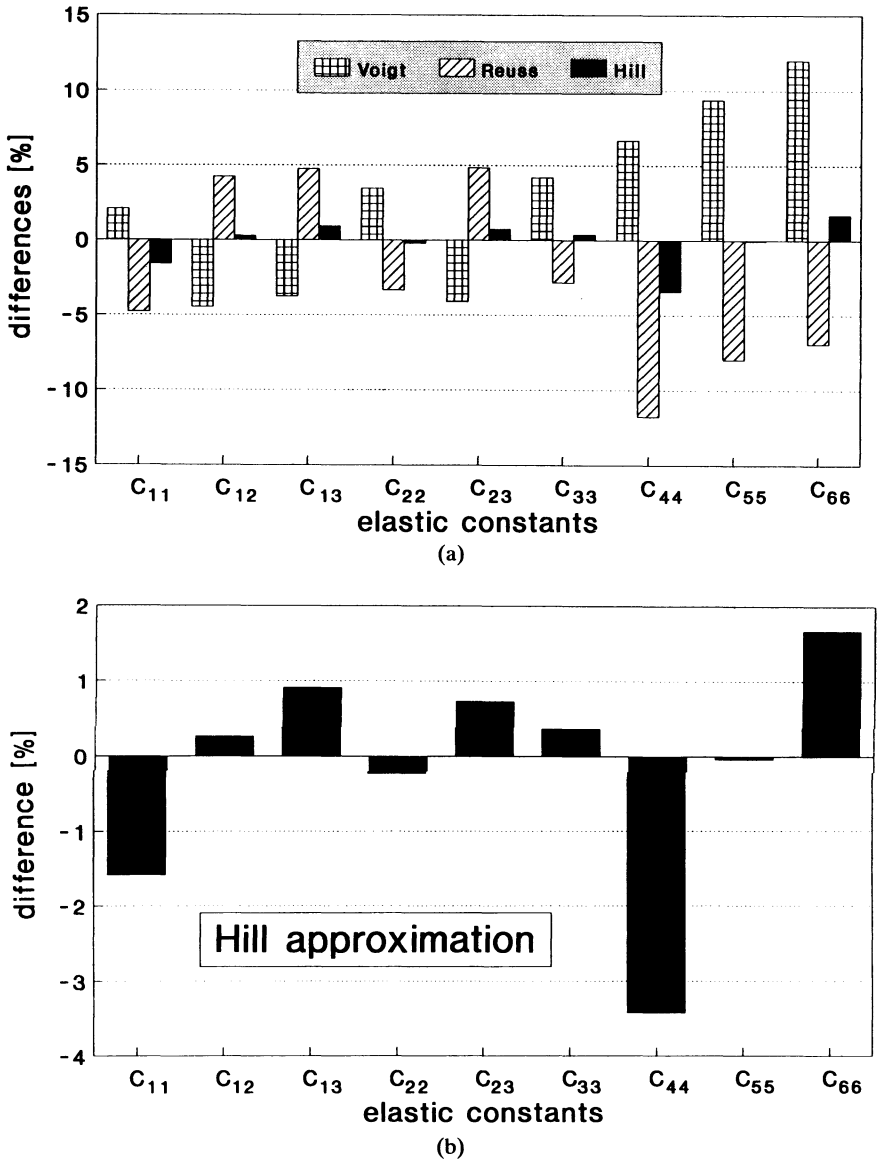

Figure 6 The differences in [%] between the elastic constants obtained from ultrasonic and texture measurements, respectively. (a) Voigt, Reuss, Hill approximation, (b) Hill approximation.

dependence of the elastic constants in the framework of non-linear elasticity theory, compressive stresses in some crystallites may increase Young's modulus more than tensile stresses decrease it in other parts of the polycrystalline material. This effect was at first formulated for two-phase materials (Bunge 1989, Ratke 1989). However, it is also to be expected in single phase materials. This contribution to the elastic properties vanishes after stress relaxation by annealing

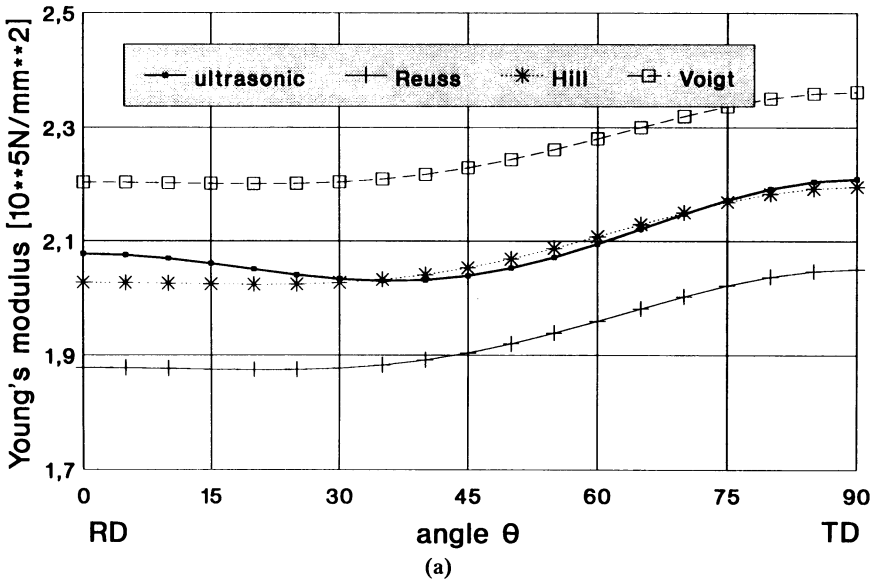

(a)

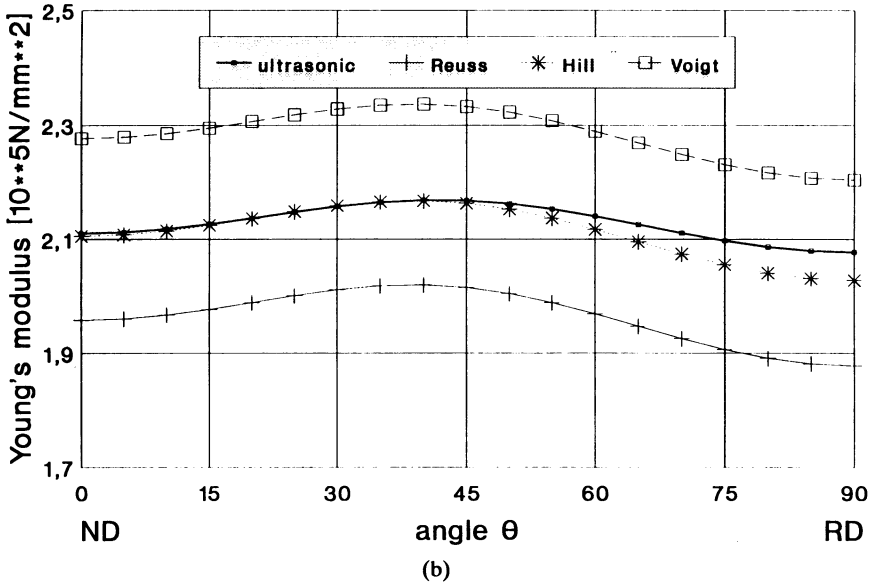

(b)

Figure 7 Young's modulus as a function of the angle θ in the three main sample planes. (a) RD-TD-plane, (b) RD-ND-plane, (c) TD-ND-plane.

as was experimentally proven (Beusse *et al.*). In the present material residual stresses did not occur to a considerable degree. The above mentioned cold rolled copper was not stress relieved. Hence, the additional part of elastic normal anisotropy observed by Bunge, Öhme and Günther may have been caused by residual stresses.

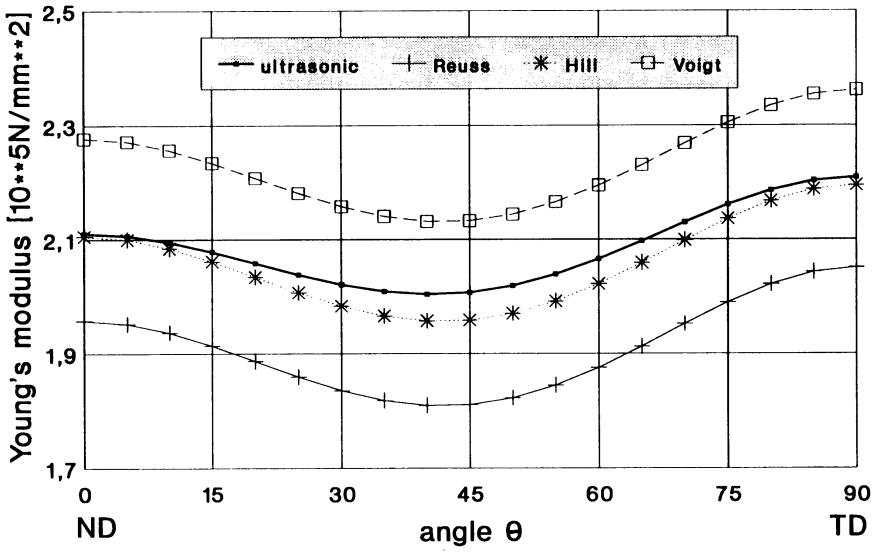

(c)

Figure 7 Young's modulus as a function of the angle θ in the three main sample planes. (a) RD-TD-plane, (b) RD-ND-plane, (c) TD-ND-plane.

References

Arndt, G. (1980). Diploma Work, TU Clausthal.

Beusse, R., Böcker, W. and Bunge, H. J.; *Scripta Met* in print.

Bunge, H. J. (1968). *Kristall u. Technik* **3,** 431–438.

Bunge, H. J. (1982). Texture Analysis in Materials Science, Butterworths Publ., London.

Bunge, H. J. (1989). *Textures and Microstructures* **10,** 153–164.

Bunge, H. J., Öhme, K. and Günther, F. (1970). *Phys. Stat. Sol.* **(a)1,** K 135–137.

Durand, G. (1977). Elements de Calcul Numerique des Fonctions de Repartion Relatives a la Representation Tridimensionelle des Textures et au Trace Automatique des Figures de Pole correspondantes, Thesis, University of Toulouse.

Green, R. E. Jr. (1973). Treatise on Materials Science and Technology, Vol. 3, *Ultrasonic Investigation of Mechanical Properties,* Academic Press, New York.

Herzer, R. and Schneider, E. (1989). In: *Nondestructive Characterization of Materials,* Eds. P. Höller, V. Hauk, G. Dobmann, C. Ruud, R. Green, Springer Verlag Berlin, 673–680.

Hill, R. (1952). *Proc. Phys. Soc.* **A65,** 349–354.

Kern, H. and Wenk, R. (1985). In: *Preferred Orientation in Deformed Metals and Rocks, Ed. H. R. Wenk, Academic Press, Orlando,* 537.

Kneer, G. (1965). *Phys. Stat. Sol.* **9,** 825–838.

Kröner, E. (1958). *Z. Phys.* **151,** 504–518.

Nye, J. F. (1975). *Physical Properties of Crystal,* Clarendon Press, London.

Ratke, L. (1989). *Textures and Microstructures* **10,** 227–242.

Reuss, A. (1929). *Z. angew. Math. Mech.* **9,** 49–58.

Voigt, W. (1928). *Lehrbuch der Kristallphysik,* B. G. Teubner Verlag, Leipzig.

Welch, P. I. (1980). *Textures and Microstructures* **2,** 99–110.

Wunnicke, W. (1986). Diploma Work, TU Clausthal.